CHEMISTRY
A European Journal

A Journal of
ChemPubSoc Europe

Accepted Article

Title: A green-LED driven source of hydrated electrons characterized from microseconds to hours and applied to cross couplings

Authors: Robert Naumann and Martin Goez

To be cited as: *Chem. Eur. J.* 10.1002/chem.201800626

Link to VoR: http://dx.doi.org/10.1002/chem.201800626

Supported by
ACES

WILEY-VCH

10.1002/chem.201800626

A green-LED driven source of hydrated electrons characterized from microseconds to hours and applied to cross couplings[†]

By Robert Naumann and Martin Goez[*]

Abstract: *We present a novel photoredox catalytic system that delivers synthetically useable concentrations of hydrated electrons when illuminated with a green light-emitting diode (LED). The catalyst is a ruthenium complex protected by an anionic micelle, and the urate dianion serves as sacrificial donor confined to the aqueous bulk. Through its chemical properties, that donor not only suppresses charge recombination that would limit the electron yield but also enables this system to perform cross couplings via hydrated electrons, for which we report the first examples. We have investigated the kinetics of all the steps involving the electron and its direct precursor in a comparative study by using laser flash photolysis and by monitoring product formation during LED photolysis. Despite the differences in timescales, each approach on its own already gives a complete picture of the reaction over a temporal range ten orders of magnitude wide. Noticeable discrepancies between the kinetic parameters obtained with the two complementary techniques can be rationalized with the slow secondary chemistry of the system; they reveal that the product-based method provides a more accurate description because it responds also to the changes of the system composition during a synthesis; hence, they demonstrate that in complex systems the timescale of the experimental observation should be matched to that of the actual application.*

1 Introduction

Photoredox catalysis with the hydrated electron $e_{aq}^{\bullet-}$ as a relay unleashes a reductive power stronger than that of most excited states, yet conveys it through an intrinsically much longer-lived intermediate (standard potential of $e_{aq}^{\bullet-}$, −2.9 V; unquenched lifetime, typically 1–2 μs)[1]. As specific "green" advantages, the attack of $e_{aq}^{\bullet-}$ on a substrate affords no by-product, and the solvent is water.

We recently found a sustainable access to $e_{aq}^{\bullet-}$ with visible light by the two-photon ionization of $[Ru(bpy)_3]^{2+}$ as the catalyst with ascorbate Asc^{2-} as a sacrificial donor.[2] When we raised the Asc^{2-} concentration to a few tens of mM, this system afforded laboratory-scale concentrations of $e_{aq}^{\bullet-}$ with single flashes from a green solid-state laser;[3] and when we additionally shielded the catalyst by an anionic micelle (of sodium dodecyl sulfate SDS), a green light-emitting diode (LED) sufficed for the same purpose,[4] which now allows employing the super-reductant $e_{aq}^{\bullet-}$ as a routine reagent, without special instrumentation, and without the safety hazards incurred by lasers or radiolysis.

This work aims at enlarging the scope of the $[Ru(bpy)_3]^{2+}$ electron source to encompass also $e_{aq}^{\bullet-}$-induced cross couplings, an objective intrinsically incompatible with ascorbate as

[*]Robert Naumann, Prof. Dr. Martin Goez,
Martin-Luther-Universität Halle-Wittenberg, Institut für Chemie, Kurt-Mothes-Str. 2, D-06120 Halle (Saale), Germany.
E-mail: martin.goez@chemie.uni-halle.de

[†]Supporting Information available: NMR spectra of additional cross couplings. See DOI: ...

the sacrificial component: the monoanion $HAsc^-$ has a pK_a of 11.74;[5] hence, even at the strongly basic pH of our experiments, 12.7, the potent hydrogen donor $HAsc^-$ is still present in mM concentrations, and thus efficiently scavenges the intermediate substrate-derived radicals before they can undergo cross coupling. To avoid this scenario, we chose the urate dianion Ur^{2-} (for the structural formula, see Figure 1b below) as a replacement. Urate is a classical water-soluble antioxidant with a lower acidity of its monoanion (pK_a, 9.8)[6] compared to $HAsc^-$. At pH 12.7, therefore, it exists practically quantitatively as Ur^{2-}, which is a good electron donor but cannot directly transfer a hydrogen atom.[7]

An equally strong motive for selecting Ur^{2-} as the sacrificial agent was an envisaged mechanistic advantage for the catalytic cycle. As discussed in detail in Section 3.1, the cornerstone for successful $e_{aq}^{\bullet-}$ production by LED illumination is a sufficiently slow recombination between the reduced catalyst and the oxidized electron donor, the former residing inside the micelle and the latter in the aqueous bulk. We expected Ur^{2-} to be favourable in this respect because its oxidized form $Ur^{\bullet-}$ possesses a pK_a of 9.5[6] and should thus be deprotonated quasi-instantaneously at pH 12.7 to give the dianionic radical $Ur^{\bullet 2-}$, which experiences a stronger Coulombic repulsion by the anionic micelle than does the singly charged $Asc^{\bullet-}$; and a further deprotonation of $Ur^{\bullet 2-}$ (p$K_a \approx 13$)[8] increases this effect even more. These electrostatic effects should thus decelerate the recombination.

As additional benefits, Ur^{2-} is similarly inexpensive and equally bioavailable as is Asc^{2-} but exhibits a much lower susceptibility to oxygen; and it remains completely transparent above 450 nm throughout the reaction whereas Asc^{2-} has a propensity to turn brown, which reduces the amount of light absorbed productively and heats up the samples at larger turnover.

Before furnishing proof of principle that the $[Ru(bpy)_3]^{2+}$ / Ur^{2-} system can effect cross couplings through $e_{aq}^{\bullet-}$, we present a comprehensive mechanistic and kinetic investigation of the reaction steps in our catalytic electron source up to and including the capture of $e_{aq}^{\bullet-}$ by a substrate. Leading photochemists have recently criticised a tendency to neglect such issues in studies on systems for photoredox catalysis, in particular with respect to the fast kinetics of the elementary processes;[9–11] on the other hand, many synthetic laboratories are not equipped for performing time-resolved photochemical experiments on the required timescales. In an attempt to help resolve this controversy, we compare the kinetics obtained by nanosecond laser flash photolysis and by monitoring the evolution of the reactant and product concentrations during preparative illumination for hours. As will emerge, the outcome is not always identical because the experiments on the short timescales do not capture the changes of the system during the course of a synthesis; but our results will show how the kinetic parameters relevant for an actual application can be obtained by experiments accessible to every laboratory.

2 Experimental

All chemicals were obtained in the highest available purity and used as received.

Nanosecond laser flash photolysis was performed with a setup described elsewhere.[3] Its relevant features include high-intensity excitation (pulse width, 5 ns) with collimated beams sent through optically thin solutions, such that absolute concentrations of transients can be

reliably measured; detection by absorption or luminescence; and a flow-through system to ensure that each laser flash hits fresh solution.

For the LED experiments, 3.8 ml of the degassed solutions were irradiated in a fluorescence cuvette with a Prizmatix UHP-T-LED-520 (maximum optical power, 1.8 W, with reproducible variation by the current source; emission maximum and full width at half maximum, 520 nm and 37 nm, closely matching the absorption maximum of OER in the visible; beam collimated to a diameter of 8 mm) under continuous stirring. The partial illumination of the sample and the volume change during the experiments were taken into account by correcting the illumination times as derived previously.[12]

After predetermined times, the LED was blocked for about 1 min while aliquots of 0.2 ml and 40 μl were removed. The concentrations of Cl^- and of remaining $[Ru(bpy)_3]^{2+}$ were determined in the former aliquot (by using an ion-sensitive electrode and the luminescence, both with the procedures described before)[4], those of Ur^{2-} by diluting the latter aliquot with 20 ml of the basic SDS medium (50 ml, pH 12.7) and recording an absorption spectrum (see, Figure 4a).

NMR product analysis at illumination endpoints was performed on an Agilent Technologies 500 MHz DD2 spectrometer and involved the same procedure as before (PRESAT pulse sequence for suppressing the intense water signal, addition of 10 % v/v of D_2O for shimming and locking, acidification to pH 1 in the case of ClAc, SDS as reference for the concentrations).[3,4]

3 Results and discussion

3.1 Mechanism and kinetics

We have already reported on the cyclic photoionization of $[Ru(bpy)_3]^{2+}$ with ascorbate Asc^{2-} as the sacrificial donor.[2–4] Because the light is only absorbed by the complex, a replacement of Asc^{2-} by urate Ur^{2-} leaves unchanged the two photoprocesses involved but modifies the intervening and subsequent thermal reactions. Figure 1a sums up the mechanism, and Figure 1b displays the formulas of the two key compounds $[Ru(bpy)_3]^{2+}$ and Ur^{2-}.

The active species of $[Ru(bpy)_3]^{2+}$ is its one-electron reduced form OER. One green photon liberates the hydrated electron $e_{aq}^{\bullet -}$ from OER with an intensity-proportional rate constant $\kappa_{ion} I$, concomitantly recovering the complex in its ground state GS, another green photon converts GS into the metal-to-ligand charge-transfer excited state ^{3}MLCT with rate constant $\kappa_{exc} I$. Electron-transfer quenching of ^{3}MLCT by the sacrificial donor (rate constant, k_q; efficiency, η; unquenched lifetime, τ_0) connects the two ends of this chain in the desired way for a catalytic cycle, whereas recombination of OER and the donor radical (rate constant, k_{rec}) competes with the electron ejection and acts as an unwanted shunt to GS.

Evidently, the ability of this mechanism to operate under the low photon flux I of an LED pivots on suppressing that recombination as much as possible. At first glance, this suggests an uphill struggle since the oxidation necessarily turns the sacrificial donor into a species with a charge more positive by one unit, hence attracted more strongly or repelled less weakly by the anionic micelle than was the donor. However, one can elegantly circumvent

10.1002/chem.201800626

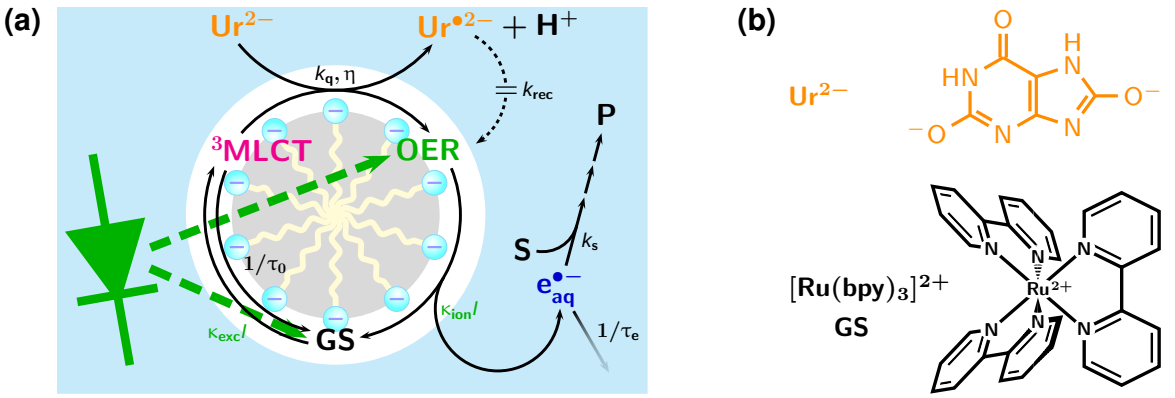

Figure 1: Mechanism of the cyclic source of hydrated electrons $e^{\bullet -}_{aq}$. Graph (a), cartoon representation of the reaction scheme. Only the catalyst $[Ru(bpy)_3]^{2+}$ in its three forms (ground state GS, metal-to-ligand charge-transfer excited state ^{3}MLCT, and one-electron reduced form OER) is solubilized by the SDS micelle; the quencher Ur^{2-}, its resulting radical $Ur^{\bullet 2-}$, and $e^{\bullet -}_{aq}$ reside exclusively in the aqueous phase. The photons from the green LED are absorbed by GS and OER. After ejection, $e^{\bullet -}_{aq}$ reacts with a hydrophilic substrate S, ultimately yielding a product P. All kinetic parameters needed for analysis with Equation 1, below, are given at the reaction arrows (in green for the light-driven steps, the rate constants of which are proportional to the LED intensity I). Graph (b), structural formulas of the catalyst $[Ru(bpy)_3]^{2+}$ in its ground state GS and of the quencher, the urate dianion Ur^{2-}.

this problem by employing Ur^{2-} because the radical produced by its oxidation possesses a pK_a of 9.5,[6] so immediately loses a proton in sufficiently basic medium (pH in all our experiments, 12.7) to give the dianionic intermediate $Ur^{\bullet 2-}$.

A first prognosis of whether a combination of $[Ru(bpy)_3]^{2+}$ with a particular quencher might qualify as an electron source should be based on the kinetic parameters k_q, η, τ_0, and k_{rec} of the two dark reactions leading to and from OER. Figure 2 collects the results obtained by laser flash photolysis for the system of this work.

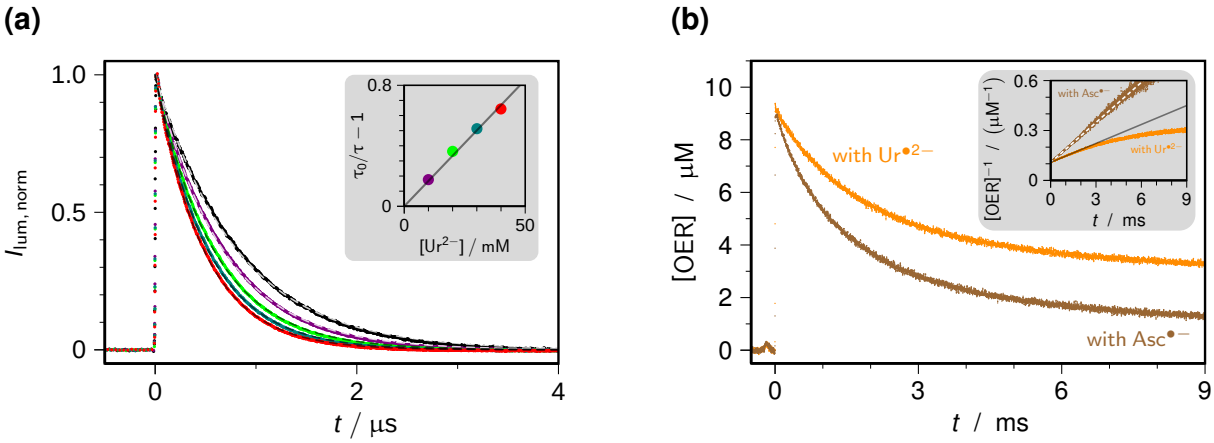

Figure 2: OER formation and decay in the system of this work (in the case of the decay also compared with Asc^{2-} as the quencher), as studied by laser flash photolysis. Common experimental conditions, 50 μM $[Ru(bpy)_3]^{2+}$ in 50 mM aqueous SDS at pH 12.7; ionic strength kept at the value with the respective maximum quencher concentration by adding Na_2SO_4; excitation with a 532 nm flash of intensity 458 mJ cm^{-2}. Graph (a), main plot; quenching of the ^{3}MLCT luminescence by Ur^{2-} (concentration in mM / colour code, 0 / black, 10 / violet, 20 / green, 30 / teal, 40 / red); traces normalized to the maximum amplitude without quencher and overlaid with best-fit functions (dashed lines) $\exp(-t/\tau)$; resulting unquenched lifetime τ_0, 780 ns. Inset, corresponding Stern–Volmer plots for Ur^{2-} using the same colour coding as in the main plot, slope of the regression line, 16.7 M^{-1}. Graph (b), OER decay in experiments with identical initial radical formation; quencher concentrations / colour code, 40 mM Ur^{2-} / orange, 18 mM Asc^{2-} / brown; main plot, experimental traces; inset, linearization for a second-order process, overlaid regression lines corresponding to rate constants of 8.0 × 10^7 M^{-1}s^{-1} ($Asc^{\bullet -}$) and 3.8 × 10^7 M^{-1}s^{-1} ($Ur^{\bullet 2-}$).

The decays of ^{3}MLCT in the presence of variable Ur^{2-} concentrations all start from the same initial value and obey clear first-order laws with rate constants exhibiting Stern–Volmer

10.1002/chem.201800626

behaviour (Figure 2a). These observations establish that Ur^{2-} quenches ^{3}MLCT purely dynamically and across the micelle-water interface in the same way as does Asc^{2-}, but with an almost three times smaller rate constant ($2.1 \times 10^7\,M^{-1}s^{-1}$) owing to its more positive standard potential (0.26 V)[6]. The good solubility in water (saturation concentration of disodium urate, about 80 mM; of dilithium urate, several hundreds of mM) facilitates compensating for this deceleration by raising the quencher concentration. We measured an efficiency η of 0.48 for OER formation with Ur^{2-}, which is almost three quarters of the value with Asc^{2-} and compares very favourably with phenolates, anilines, thiocarbamate or cysteine, none of which we found to reach a higher η than 0.2. Owing to the long unquenched lifetime of ^{3}MLCT (τ_0, 0.78 μs), our standard concentration of Ur^{2-} (40 mM) thus suffices for producing one molecule of OER for every fifth photon.

The recombination of OER and the quencher-derived radical plays an even more important role than does the ^{3}MLCT quenching because it determines the storage duration and hence the probability of absorbing the ionizing photon. Decisive are not only a low rate constant but also a reaction order higher than first order.[4] Figure 2b juxtaposes decay traces of OER accessed through ^{3}MLCT quenching by Ur^{2-} and Asc^{2-}, where the quencher concentrations were chosen such as to produce identical initial amounts in both systems. Direct observation at a wavelength practically coinciding with the OER absorption maximum is possible because all quencher-derived species are transparent in this spectral range[4,6] while ^{3}MLCT and GS are blanked through having an isosbestic point. As is immediately perceived, OER recombines significantly more slowly with $Ur^{\bullet 2-}$ than with $Asc^{\bullet -}$, which proves our strategy of compensating the more positive charge on the quencher radical by a subsequent deprotonation to be workable. What is more, the inset of Figure 2b reveals systematic and progressive deviations of the OER/$Ur^{\bullet 2-}$ recombination from second-order kinetics at longer times such that the OER decay becomes increasingly slower and has almost come to a halt at the end of the observation period. This effect is seen to be absent on the same (10 ms) timescale when Asc^{2-} is the sacrificial donor, and we ascribe it to a faster removal of $Ur^{\bullet 2-}$ from the system by disproportionation than in the case of $Asc^{\bullet -}$.

These encouraging results prompted us to investigate the performance of this system with the chloroacetate assay. This assay is specific through neither responding to reductants weaker than $e^{\bullet -}_{aq}$ nor poisoning catalysts solubilized in SDS micelles; moreover, it directly corresponds to an environmentally relevant application. The reaction scheme is displayed in Figure 3a. The highly toxic chloroacetate ClAc captures $e^{\bullet -}_{aq}$ with a rate constant in excess of $10^9\,M^{-1}s^{-1}$, the exact value depending on the ionic strength of the solution. The electron attachment is dissociative and results in the harmless chloride ion and the carboxymethyl radical, which finally stabilizes to give the equally innocuous acetate Ac. As illustrated by the NMR spectra shown in the Figure, exhaustive illumination of 1 mole percent of the catalyst destroyed most (> 95 %) of the substrate ClAc with practically complete recovery as Ac; the amount of the radical combination product succinic acid was negligible (< 1 %). However, considerably more information than from the system composition at the end point is obtained from the development of the concentrations during the illumination period. Figures 3b and 4a collect this for the catalyst and Cl^-, as well as for the sacrificial donor. The analysis involves discontinuous operation: the illumination of the samples is interrupted at certain times to remove small aliquots, and the associated reduction of the sample volumes is taken into account by correcting the duration of the subsequent illumination.

10.1002/chem.201800626

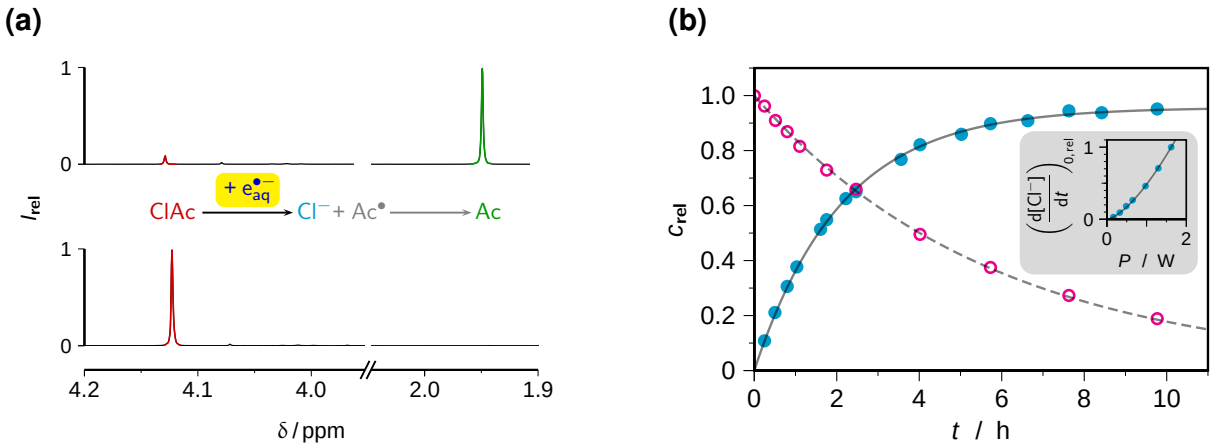

Figure 3: Characterizing the catalytic electron source with the chloroacetate assay. System composition, 0.1 mM $[Ru(bpy)_3]^{2+}$ and 40 mM Ur^{2-} in 50 mM aqueous SDS at pH 12.7; 10 mM chloroacetate ClAc. Graph (a), NMR spectra with identical vertical scales before (bottom trace) and after (top trace) illumination for 10 h with a green LED (520 nm). The toxic ClAc (red singlet, 4.12 ppm) is converted near-quatitatively into the harmless acetate Ac (green singlet, 1.94 ppm) as shown by the reaction scheme between the traces. Graph (b), kinetics during the experiment of graph (a). Main plot, relative concentrations of liberated chloride ions (cyan filled circles and solid fit curve $0.954\{1 - \exp[-t/(2.08\,\mathrm{h})]\}$) and of remaining catalyst (magenta open circles and dashed fit curve $\exp[-t/(5.79\,\mathrm{h})]$); inset, relative initial slope of Cl^- production as function of the LED radiative power P, with fit curve $[P/(1.62\,\mathrm{W})]^{3/2}$.

The catalyst concentration can be monitored conveniently and selectively through the ^{3}MLCT luminescence, after dilution and acidification to eliminate quenching by the sacrificial donor or its oxidation products; and the Cl^- concentration can be determined without interference from other species by using an ion-sensitive electrode. As is seen in Figure 3b, the time dependences of the $[Ru(bpy)_3]^{2+}$ and Cl^- concentrations are excellently representable by monoexponential functions; but the observation that this is only possible individually, with best-fit rate constants differing by a factor of nearly three, already exposes this simplicity as deceptive and rules out any direct interpretation of the fit parameters. Because the evolution of the system comprises negative feedback between the concentrations of the key species,[4] and because the secondary chemistry of the sacrificial donor is only rudimentarily known, the initial slopes are the only observables on which conclusions should be based; and even in this temporal range, the system composition is not completely certain, as will emerge below.

With the kinetic parameters of Figure 1a, the initial rate of Cl^- formation can be expressed as the product of three terms p, q, and r,[4] each of which describes the dependence on an easily varied quantity (p, light intensity I; q, quencher concentration [Q], Q = Ur^{2-} or Asc^{2-} this work; r, substrate concentration [S], S = ClAc with the chloroacetate assay). The abbreviation Cat stands for $[Ru(bpy)_3]^{2+}$, and all concentrations on the r.h.s. of Equation 1 are weight-in concentrations.

$$\left(\frac{d[Cl^-]}{dt}\right)_{t=0} = p \times q \times r \qquad (1)$$

$$= \left(I^{3/2}\kappa_{ion}\sqrt{\frac{\kappa_{exc}[Cat]\,\eta}{k_{rec}}}\right) \times \left(1 + 1/(k_q\tau_0[Q])\right)^{-1/2} \times \left(1 + 1/(k_s\tau_e[S])\right)^{-1}$$

The inset of Figure 3b demonstrates that the $e^{\bullet}_{aq}$ yield is indeed proportional to $I^{3/2}$, because the intensity I is proportional to the LED radiative power P in turn. This characteristic

10.1002/chem.201800626

dependence identifies the mechanism as being cyclic and featuring the monophotonic ionization of a catalyst form that is itself produced by a monophotonic reaction and reverts to the starting state by a second-order dark process. The term p also provides a criterion for the selection of the LED: κ_{exc} and κ_{ion} are proportional to the extinction coefficients of OER and GS at the LED wavelength,[13] but their different exponents make it much more important to match the LED emission to the spectrum of the direct electron precursor OER; and this is intensified by the fact that κ_{exc} and κ_{ion} are also proportional to the quantum yield of the respective process,[13] which is unity for the primary excitation but only a few percent for electron ejection.

Figure 4 focuses on the influence of the quencher. To quantify the amount of remaining Ur^{2-}, we had to use an approach different from that in our earlier study with Asc^{2-} as the sacrificial donor, because the Folin–Ciocalteu reagent employed there also responds to the oxidation products of Ur^{2-}. Instead, the intense absorption of Ur^{2-} in the UV-B (λ_{max} = 295 nm, ε_{max} = 13200 $M^{-1}cm^{-1}$; see, main plot of Figure 4a) turned out to be well suited for the purpose. Interference from the catalyst-based species also absorbing there plays no role on account of the large disparity of concentrations; and scaling each spectrum to maximum reveals that the band shape at $\lambda \geq \lambda_{max}$ remains invariant during the reaction, thus ruling out a superposition of absorptions of different species in this range.

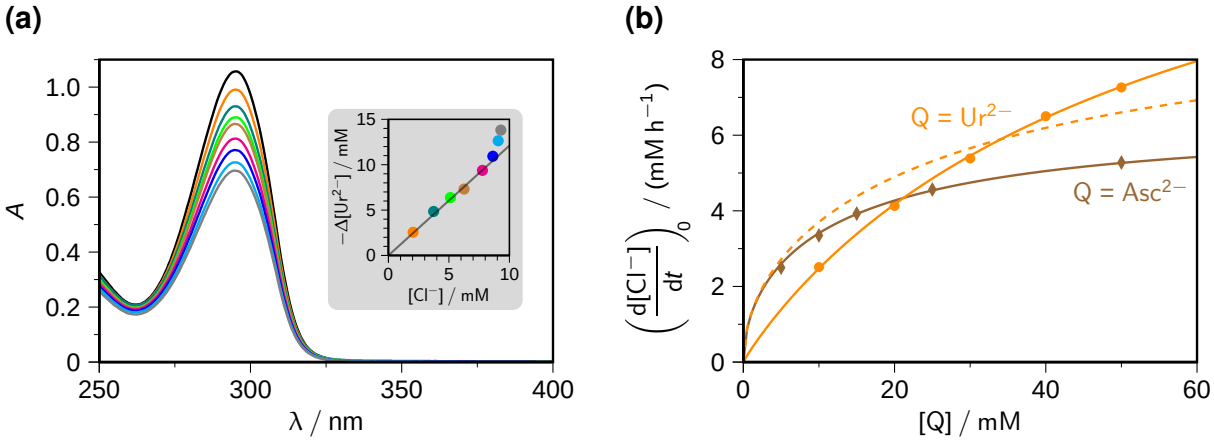

Figure 4: Consumption during, and effect of the quencher on, Cl^- production with the ClAc assay. Graph (a), development of $[Ur^{2-}]$ during the experiment of Figure 3; main plot, UV spectra recorded at different illumination times; inset, Ur^{2-} decrease (obtained by integrating the spectra of the main plot between 295 nm and 315 nm) as function of Cl^- increase with regression line of slope 1.2, same colour code for the data points as for the Ur^{2-} bands as in the main plot. Graph (b), initial slope of chloride formation in experiments as in Figure 3 but with 50 mM ClAc, x mM of quencher Q and (50 − x) mM Na_2SO_4 for keeping the ionic strength constant. The data for Asc^{2-} (brown, diamonds, solid fit curve) can be represented by q (Equation 1) with $k_q\tau_0$ = 37.7 M^{-1}, which is the Stern–Volmer constant obtained from laser flash photolysis at this ionic strength, whereas the data for Ur^{2-} (orange, circles) differ widely from the corresponding curve (dashed; $k_q\tau_0$ = 16.7 M^{-1} from Figure 2a) and can only be accommodated with this Stern–Volmer constant when the exponent in q is set to −0.933 (orange solid curve).

The conversion of ClAc into Ac theoretically requires two molecules of the sacrificial donor, the first serving as an electron donor for generating the $e^{\bullet-}_{aq}$ precursor OER, and the second as a hydrogen donor for intercepting the carboxymethyl radical (compare, the scheme in Figure 3a). Both with Asc^{2-} and with Ur^{2-}, donor consumption is indeed found to be proportional to substrate consumption (as measured by chloride formation) during most of the reaction, up to 95 % and 80 % turnover; but the constant of proportionality amounts to only 1.6 in the case of Asc^{2-} and to only 1.2 in the case of Ur^{2-} (see, the inset of Figure 4a). We ascribe the deviations to the disproportionation of two donor-based radical, which

10.1002/chem.201800626

recovers one molecule of the donor. For $Asc^{\bullet-}$, this reaction has been investigated in some detail,[5] whereas for $Ur^{\bullet 2-}$ it is known but has largely remained unexplored.[14] Depending on what fraction of the radicals undergoes disproportionation, any constant of proportionality between 1 and 2 can be rationalized, and the experimental observation puts this fraction at 40 % for $Asc^{\bullet-}$ and at 80 % for $Ur^{\bullet 2-}$. A larger amount of Ur^{2-} recycling is also consistent with Figure 2b, which revealed that the recombination of OER with $Ur^{\bullet 2-}$ — as opposed to that with $Asc^{\bullet-}$ — started noticeably to deviate from a second-order process already after 4 ms, as it must when $Ur^{\bullet 2-}$ is consumed by another process.

This discrepancy between the short-time kinetics with Asc^{2-} and Ur^{2-} in Figure 2b is reflected by the long-time behaviour observed through the dependence of the initial Cl^- formation rate on the quencher concentration in Figure 4b. In these experiments, the ClAc concentration was chosen so high that the deviations of the term r (Equation 1; see the discussion below) from unity are insignificant throughout the range of [Q]. The data for Asc^{2-} with its regular second-order OER decay are perfectly accommodated by the term q with the parameters extracted from measurements as in Figure 2, in other words, the laser-flash photolysis results are sufficient for anticipating the outcome under preparative photolysis. But the same dependence on $[Ur^{2-}]$ is not only impossible to fit with the corresponding kinetic parameters from the short-time experiments but also generally impossible to fit with the inverse square-root law for q when the value of $k_q\tau_0$ is positive, as it must be; the only way to reproduce the data with the known Stern–Volmer parameter is by increasing the exponent to almost unity. Hence, in this system a complex secondary chemistry renders flash photolysis useless for making quantitative predictions for LED photolysis; but experiments on short timescales still retain their value for establishing whether or not $e_{aq}^{\bullet-}$ formation is feasible in principle.

Figure 5 pinpoints a related divergence with respect to the electron capture by the substrate (the term r in Equation 1). This process has to compete with the $e_{aq}^{\bullet-}$ decay through all other channels, amongst which the reaction with the sacrificial donor plays a major role on account of its high concentration even though donors are intrinsically inefficient $e_{aq}^{\bullet-}$ scavengers. As can be seen in Figure 5a, $e_{aq}^{\bullet-}$ generated by laser flashes on the $[Ru(bpy)_3]^{2+}/Ur^{2-}$ system in the absence of ClAc vanishes through a pseudo first-order process exhibiting Stern–Volmer behaviour when the Ur^{2-} concentration is varied. The relatively low rate constant of $9.0 \times 10^7\,M^{-1}s^{-1}$ and long unquenched $e_{aq}^{\bullet-}$ lifetime of 0.81 μs obtained from these experiments are in line with expectation, and predict the much more efficient $e_{aq}^{\bullet-}$ scavenger ClAc (rate constant k_S of electron capture, about $1.8 \times 10^9\,M^{-1}s^{-1}$ at the high ionic strength of these systems) to compete successfully.

As Figure 5b demonstrates, this is indeed the case. However, keeping τ_e in the function r fixed at the values from laser flash photolysis gave poor fits of the dependences on the substrate concentration, with deviations that were already noticeable in the case of Asc^{2-} and clearly inacceptable in that of Ur^{2-}. Good representations were only obtained when τ_e was treated as an adjustable quantity, and the fits converged on values of τ_e that were shorter by factors of 1.8 and 2.8 than those extracted from the measurements on μs timescales.

We ascribe the contradictions between these observations on short and long timescales to the same cause as those between Figures 2b and 4b: soon after the start of the illumination — with Ur^{2-} already within ms, as evidenced by the inset of Figure 2b — the secondary chemistry of the donor radicals sets in, so the LED experiments experience the

10.1002/chem.201800626

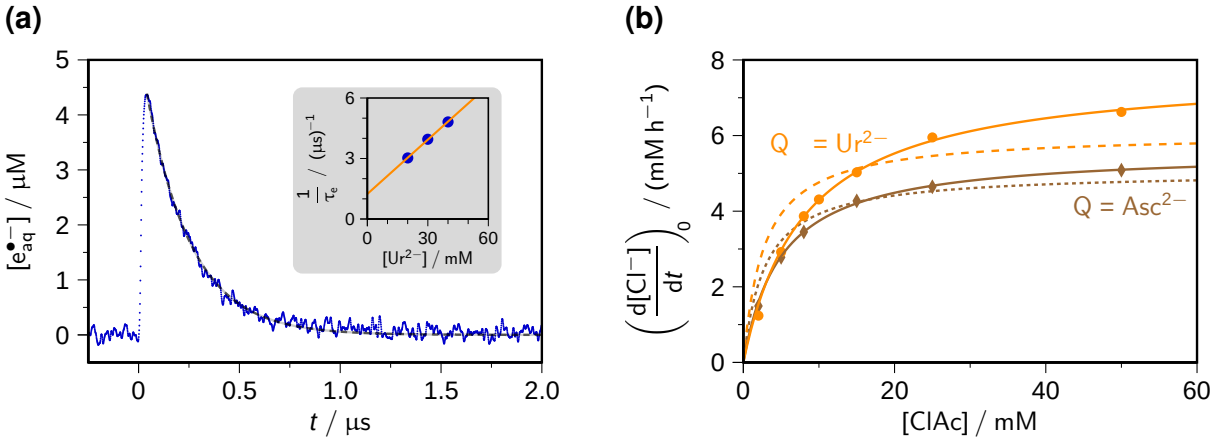

Figure 5: Capture of $e_{aq}^{\bullet-}$ investigated by experiments on different timescales. Common conditions, 0.1 mM $[Ru(bpy)_3]^{2+}$ in 50 mM aqueous SDS at pH 12.7, ionic strength in each series of measurements kept constant by adding the required amount of Na_2SO_4. Graph (a): main plot, $e_{aq}^{\bullet-}$ trace in the presence of 40 mM Ur^{2-}, $e_{aq}^{\bullet-}$ generation by laser flash photolysis (532 nm) with the sequence flash (412 mJ cm^{-2}) — delay (5 μs) — flash (664 mJ cm^{-2}) at 0 μs, overlaid with dashed fit curve $a\exp(-t/\tau_e)$ with best-fit value 207 ns for τ_e; inset, Stern–Volmer plot based on τ_e giving an unquenched $e_{aq}^{\bullet-}$ lifetime (from the intercept) of 805 ns and a rate constant for $e_{aq}^{\bullet-}$ scavenging by Ur^{2-} of 9.0×10^7 M^{-1}s^{-1}. Graph (b), initial slope of Cl^- formation from variable amounts of ClAc, concentration of the sacrificial donor Q fixed at 75 mM (Asc^{2-}, brown, diamonds) or 40 mM (Ur^{2-}, orange, filled circles). The solid lines are fit curves of r (Equation 1) with adjustable amplitude and $k_S\tau_e$ (best-fit values / independently determined k_S at the pertaining ionic strength / resulting τ_e, 201 M^{-1} / 1.9×10^9 M^{-1}s^{-1} / 106 ns for Asc^{2-} and 124 M^{-1} / 1.7×10^9 M^{-1}s^{-1} / 73 ns for Ur^{2-}). The dashed lines show the best-fit curves when τ_e is kept fixed at the respective value from laser flash photolysis (Asc^{2-}, 186 ns; Ur^{2-}, 207 ns).

additional influence of species and reactions that did not exist in most laser flash photolysis traces, which are normally limited to some ten ms to avoid distortions by convection. This emphasizes the necessity of characterizing the catalytic systems on a timescale comparable to that of their application. Nevertheless, laser flash photolysis is still extremely important because it isolates, and is thus instrumental in better understanding, the "early" reactions. In particular, it will spot a sacrificial donor that does not quench ^{3}MLCT rapidly and productively enough, or one whose radical recombines too fast with OER; hence, it will help avoid fruitless optimization attempts of systems that are intrinsically useless as $e_{aq}^{\bullet-}$ sources.

3.2 Application to cross couplings

The preceding Section has shown that the $[Ru(bpy)_3]^{2+}$ / Ur^{2-} / SDS electron source is capable of delivering mM concentrations of $e_{aq}^{\bullet-}$ upon illumination with a green LED. The attack of $e_{aq}^{\bullet-}$ on chlorinated and even fluorinated aliphatic or aromatic substrates effects ejection of the halide anion; the remaining carbon-centered radical abstracts a hydrogen atom when a suitable donor is present.[3,4] Although such an exchange of halogen against hydrogen is of general importance for syntheses and environmental remediation,[15–19] the use of the intermediate radicals as building blocks in cross-coupling reactions is even more interesting.[20–24]

What would thwart such cross couplings obviously is the competitive transfer of a hydrogen atom, and in this regard Ur^{2-} as sacrificial species brings a decisive advantage over Asc^{2-} because its second pK_a is lower by two units, so at the pH of our experiments the concentration of the hydrogen-donating monoanion is a hundred times smaller than in the case of Asc^{2-}.

Especially promising as coupling reagents are *N*-alkylated pyrroles because they are

10.1002/chem.201800626

very reactive towards radicals and exclusively afford 2-substituted products; hence, even at moderate concentrations they allow an effective and selective radical usage.[25–30] In our strongly basic aqueous solutions, *N*-methyl-2-pyrrolecarboxylic acid (NMPCA) is particularly well suited for intercepting the $e_{aq}^{\bullet-}$-generated radicals, as it combines this reactivity with an excellent solubility while the deprotonated carboxylate substituent increases its hydrophilic such as to safely avoid its entry into the micelles where it might interfere with the electron source.

Figure 6a demonstrates the successful cross coupling of NMPCA with ClAc as the radical precursor to give 5-(2-carboxymethyl)-*N*-methylpyrrole-2-carboxylate **1** (for the formulas of all cross-coupling products, see Scheme 1) in moderate yield (41 %), with the system composition in the Figure — as for all the examples that follow — already representing an optimum. Together with a substantial amount of acetate formation (26 %), which reflects that even a weak hydrogen donor or one present in low concentration can compete with the slow scavenging of the carboxymethyl radical by aromatic systems, this is identical with the ClAc consumption (67 %). The incomplete consumption is a direct consequence of the known trade-off between ClAc decomposition and turnover number.[3] Increasing the NMPCA concentration does not improve the cross-coupling yield because we found that this slightly activated heteroarene can also scavenge $e_{aq}^{\bullet-}$ to give a dihydropyrrole; this reaction diminishes the fraction of $e_{aq}^{\bullet-}$ forming carboxymethyl radicals. Furthermore, the addition of NMPCA raises the ionic strength of the solution, which increases k_{rec} through the Brønsted–Bjerrum relationship,[31] so diminishes the $e_{aq}^{\bullet-}$ generation rate.

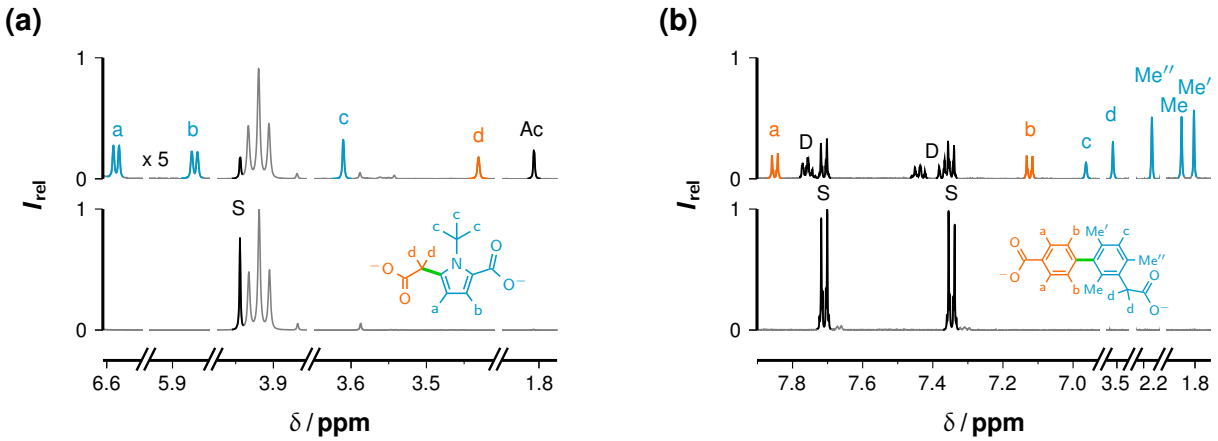

Figure 6: Cross couplings induced by $e_{aq}^{\bullet-}$. Common experimental parameters of the $e_{aq}^{\bullet-}$ source, 100 μM $[Ru(bpy)_3]^{2+}$, 40 mM Ur^{2-}, pH 12.7, 50 mM SDS. Shown are the ^{1}H-NMR spectra, with identical vertical scales before (bottom trace) and after (top trace) illumination for 14 h with a green LED, as well as the structural formula of the respective coupling product. Colour code in both spectra and formulas, orange (moiety of the $e_{aq}^{\bullet-}$-generated radical source) and cyan (radical-scavenger moiety); in the spectra only, black (radical source S and product derived from S without participation of the radical scavenger). Graph (a), 10 mM ClAc (3.95 ppm, s; hydrogen-abstraction product Ac, 1.81 ppm, s) and 100 mM NMPCA. Cross-coupling product 5-(2-carboxymethyl)-*N*-methylpyrrole-2-carboxylate; a, 6.60 ppm, d; b, 5.88 ppm, d; c, 3.62 ppm, s; d, 3.43 ppm, s. The prominent gray signal is due to SDS (3.92 ppm, t). Graph (b), 5 mM ClBz (7.71 ppm, d, and 7.35 ppm, d; dehalogenation and dimerization products D, 7.76, 7.44, and 7.37 ppm, all m) and 100 mM MesAc. Cross-coupling product 3-(4-carboxyphenyl)-mesitylacetate; a, 7.85 ppm, d; b, 7.12 ppm, d; c, 6.96, s; d, 3.51 ppm, s; Me″, 2.18 ppm, s; Me, 1.84 ppm, s; Me′, 1.80 ppm, s.

In line with this reasoning, using a much more reactive phenyl σ radical in place of the carboxymethyl radical promotes the cross coupling. The reducing power of $e_{aq}^{\bullet-}$ easily cleaves aromatic carbon–chlorine bonds,[3,4,32,33] so allowed replacing ClAc with 4-chlorobenzoate ClBz, which at halved concentrations of both the radical souce and the heteroarene raised

10.1002/chem.201800626

the yield of the cross-coupling product 5-(4-carboxyphenyl)-*N*-methylpyrrole-2-carboxylate **4** to 60 %. (For the NMR spectra, see Supporting Figure 1a.) The by-products, mainly benzoate, accounted for a further 25 %. The presence of the coupling reagent is very beneficial in this system, as in its absence the phenyl radicals also attack the catalyst, which decreases the ClBz turnover from 85 % to 37 % under otherwise identical conditions. The contrast to ClAc, where no such catalyst poisoning is observed, conspicuously demonstrates the reactivity difference between the phenyl and carboxymethyl radicals.

Omitting the carboxylate group from the pyrrole should increase the cross-coupling efficiency through lowering the propensity of the heteroarene to scavenge $e_{aq}^{\bullet-}$ parasitically and through avoiding an increase of the ionic strength. These motivations and the good solubility of the unsubstituted *N*-methyl pyrrole NMP in water prompted us employ NMP as coupling reagent for the same phenyl radical as above. Contrary to expectation, however, the NMR spectra collected in Supporting Figure 1b revealed a decrease in the yield of the cross-coupling product 2-(4-carboxyphenyl)-*N*-methylpyrrole **3** to 30 %, which is not due to increased by-product formation but results from a reduction of the ClBz turnover to 56 %. Evidently, NMP either interferes with the $e_{aq}^{\bullet-}$ generator itself or intercepts $e_{aq}^{\bullet-}$ in a nonproductive parasitic process.

A hydrophilic coupling reagent with very little tendency to scavenge $e_{aq}^{\bullet-}$ is mesitylacetate MesAc, owing to the isolation of the carboxylate function from the ring by a saturated carbon.[3] Although the considerable steric hindrance by its substituents must decelerate the attack by phenyl radicals, the cross-coupling product 3-(4-carboxyphenyl)-mesitylacetate **2** is still formed with a yield of 30 %, as the NMR spectrum of Figure 6b demonstrates, but the correspondingly longer life of the radicals results in faster catalyst poisoning, which manifests itself by a ClBz turnover of only 58 %.

Scheme 1 summarizes the $e_{aq}^{\bullet-}$-induced cross couplings described in this Section. General regularities that allow an optimization are as follows. As expected,[4] the catalyst concentration exerts no influence on the product distribution but determines the amount of $e_{aq}^{\bullet-}$ formed and the turnover rate. This is valuable with respect to synthetic output but less so from the point of view of efficient catalyst use. Increasing the substrate concentration maximizes $e_{aq}^{\bullet-}$ utilization but reduces the percentage of substrate conversion;[3] hence, although the cross-coupling product is formed in a larger absolute amount, its yield with respect to the substrate decreases. This effect can be countered by adding the substrate in several smaller portions distributed over the reaction duration. The concentration of the trapping reagent is subject to a trade-off: higher concentrations accelerate the coupling but increase the amount of parasitic $e_{aq}^{\bullet-}$ scavenging; both factors obviously influence the product yield in opposite ways.

The Ur^{2-} concentration is the only one that significantly affects the partitioning of the substrate radicals between hydrogen addition and coupling with the trapping reagent. The latter reaction channel is favoured by lowering the Ur^{2-} concentration, and this dependence becomes more prominent for a sterically hindered trapping reagent such as MesAc. When the electron generator is fuelled by ascorbate instead of urate, none of the reactions of Scheme 1 give an appreciable yield; instead, only hydrogenation products are observed. These observations clearly identify the concentration, and above all hydrogen-donating ability, of the sacrificial donor as the controlling factor, thus confirm the starting hypothesis of this work.

10.1002/chem.201800626

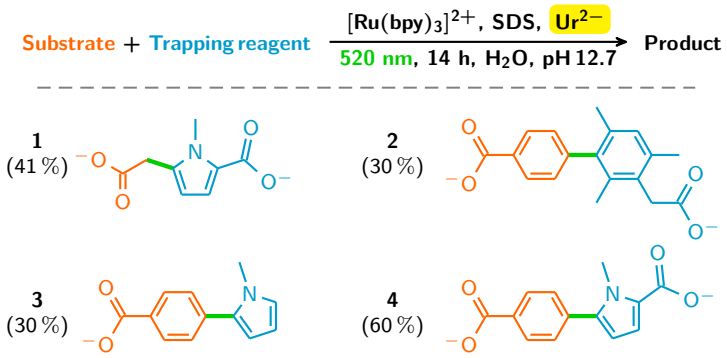

Scheme 1: Cross couplings induced through LED-generated $e^{\bullet-}_{aq}$.

4 Conclusions

With regard to mechanism and kinetics, our results have provided clear evidence that laser flash photolysis with detection on short timescales does not always provide sufficient information on the inner workings of a photoredox catalytic cycle. Such experiments are by necessity restricted either to the pristine starting state of the system (e.g., for investigating the processes surrounding the quenching step) or to an assumed and idealized intermediate state (e.g., when studying the competition between the natural decay of $e^{\bullet-}_{aq}$ and its capture by a substrate). Not accessible to them are the much slower changes during continuous illumination for periods at least a billion times longer, in particular the variation of the system composition by the secondary chemistry of the sacrificial donor; but these changes can significantly influence the fast reactions through the presence of newly formed species. Analyzing the initial slopes of product formation and catalyst decay during low-intensity preparative photolysis matches the observation window much more closely to the time frame of the actual benchtop procedure.

In addition, this work has demonstrated for the first time that $e^{\bullet-}_{aq}$ can also be enlisted as a reagent for achieving cross-couplings. With its impressive reducing power, $e^{\bullet-}_{aq}$ is not deterred by aliphatic or aromatic carbon–chlorine bonds,[4] so extends the palette of substrates that can be employed. Yet, our electron generator itself is driven by a low-power green LED; and it is sustainable because it only consumes the ubiquitous antioxidant urate. The present study has successfully validated our hypothesis that the much lower hydrogen-donating ability of the urate dianion compared to the ascorbate dianion is instrumental in suppressing the substitution of halogen by hydrogen in favour of the desired cross couplings. It has provided proof of principle by focussing on the role of the sacrificial donor, but we envisage that tuning the photocatalyst will further optimize the yields of the cross-coupling products.

References

[1] G. V. Buxton, C. L. Greenstock, W. P. Heiman, A. B. Ross, *J. Phys. Chem. Ref. Data* **1988**, *17*, 513–886.

[2] M. Goez, C. Kerzig, R. Naumann, *Angew. Chem. Int. Ed.* **2014**, *53*, 9914–9916.

[3] R. Naumann, C. Kerzig, M. Goez, *Chem. Sci.* **2017**, *8*, 7510–7520.

[4] R. Naumann, F. Lehmann, M. Goez, *Angew. Chem. Int. Ed.* **2018**, *57*, 1078–1081.

[5] M. B. Davies, J. Austin, D. A. Partridge, *Vitamin C: Its Chemistry and Biochemistry*, The Royal Society of Chemistry, Cambridge, 1st ed., **1991**.

[6] M. G. Simic, S. V. Jovanovic, *J. Am. Chem. Soc.* **1989**, *111*, 5778–5782.

[7] L. Muñoz-Rugeles, A. Galano, J. R. Alvarez-Idaboy, *Phys. Chem. Chem. Phys.* **2017**, 15296–15309.

[8] J. P. Telo, *Org. Biomol. Chem.* **2003**, *1*, 588–592.

[9] S. P. Pitre, C. D. McTiernan, J. C. Scaiano, *Acc. Chem. Res.* **2016**, *49*, 1320–1330.

[10] R. Martinez-Haya, M. A. Miranda, M. L. Marin, *Eur. J. Org. Chem.* **2017**, 2164–2169.

[11] M. Marchini, G. Bergamini, P. G. Cozzi, P. Ceroni, V. Balzani, *Angew. Chem. Int. Ed.* **2017**, *56*, 2–4.

[12] T. Kohlmann, R. Naumann, C. Kerzig, M. Goez, *Photochem. Photobiol. Sci.* **2017**, *16*, 1613–1622.

[13] M. Goez, V. Zubarev, *Chem. Phys.* **2000**, *256*, 107–116.

[14] G. L. Squadrito, R. Cueto, A. E. Splenser, A. Valavanidis, H. Zhang, R. M. Uppu, W. A. Pryor, *Arch. Biochem. Biophys.* **2000**, *376*, 333–337.

[15] L. Huang, W. B. Dong, H. Q. Hou, *Chem. Phys. Lett.* **2007**, *436*, 124–128.

[16] H. Park, C. D. Vecitis, J. Cheng, W. Choi, B. T. Mader, M. R. Hoffmann, *J. Phys. Chem. A* **2009**, *113*, 690–696.

[17] X. Li, J. Ma, G. Liu, J. Fang, S. Yue, Y. Guan, L. Chen, X. Liu, *Environ. Sci. Technol.* **2012**, *46*, 7342–7349.

[18] Y. Peng, S. He, J. Wang, W. Gong, *Radiat. Phys. Chem.* **2012**, *81*, 1629–1633.

[19] Z. Song, H. Tang, N. Wang, L. Zhu, *J. Hazard. Mater.* **2013**, *262*, 332–338.

[20] J. M. R. Narayanam, C. R. J. Stephenson, *Chem. Soc. Rev.* **2011**, *40*, 102–113.

[21] C. K. Prier, D. A. Rankic, D. W. C. MacMillan, *Chem. Rev.* **2013**, *113*, 5322–5363.

[22] *Chemical Photocatalysis*, (Ed.: B. König), DeGruyter, Berlin, **2013**.

[23] M. Reckenthäler, A. G. Griesbeck, *Adv. Synth. Catal.* **2013**, *355*, 2727–2744.

[24] N. A. Romero, D. A. Nicewicz, *Chem. Rev.* **2016**, *116*, 10075–10166.

[25] Y. M. Osornio, R. Cruz-Almanza, V. Jiménez-Montaño, L. D. Miranda, *Chem. Commun.* **2003**, 2316–2317.

[26] O. Guadarrama-Morales, F. Méndez, L. D. Miranda, *Tetrahedron Lett.* **2007**, *48*, 4515–4518.

[27] C. Iuga, S. O. Uribe, L. D. Miranda, A. Vivier-Bunge, *Int. J. Quantum Chem.* **2010**, *110*, 697–705.

[28] L. Marzo, I. Ghosh, F. Esteban, B. König, *ACS Catal.* **2016**, *6*, 6780–6784.

[29] J. I. Bardagi, I. Ghosh, M. Schmalzbauer, T. Ghosh, B. König, *Eur. J. Org. Chem.* **2018**, 34–40.

[30] M. Neumeier, D. Sampedro, M. Májek, V. A. de la Peña O'Shea, A. Jacobi von Wangelin, R. Pérez-Ruiz, *Chem. Eur. J.* **2018**, *24*, 105–108.

[31] A. A. Frost, R. G. Pearson, *Kinetics and Mechanism*, John Wiley and Sons, New York, 2nd ed., **1961**.

[32] V. V. Konovalov, S. S. Laev, I. V. Beregovaya, L. N. Shchegoleva, V. D. Shteingarts, Y. D. Tsvetkov, I. Bilkis, *J. Phys. Chem. A.* **2000**, *104*, 352–361.

[33] R. Zona, S. Solar, N. Getoff, K. Sehested, J. Holcman, *Radiat. Phys. Chem.* **2008**, *77*, 162–168.

10.1002/chem.201800626

Table of contents entry

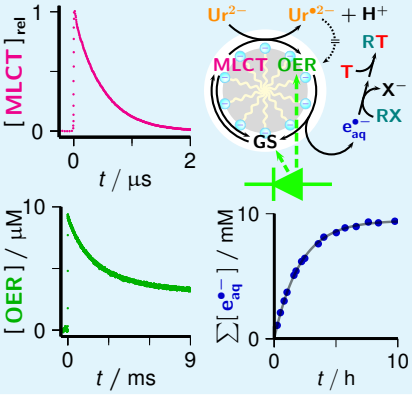

Ur the one... from microseconds to hours. A photoredox catalytic system driven by a green LED, consuming only the bioavailable urate dianion Ur^{2-} and producing hydrated electrons $e^{\bullet-}_{aq}$ is characterized over timescales spanning ten orders of magnitude, and is employed to achieve the first cross couplings induced by the super-reductant $e^{\bullet-}_{aq}$.

Keywords: Photocatalysis; Photochemistry; Sustainable Chemistry; Radical reactions; Hydrated electrons